Original article

IMAGE QUALITY IN ABDOMINAL CT: A COMPARISON OF TWO RECONSTRUCTION ALGORITHMS IN FILTERED BACK PROJECTION (FBP)

Albertina RUSANDU[1,*] Adrian BECK[2], Atle HEGGE[2], Gabriele ENGH[2]

[1] Norwegian University of Science and Technology, Department of Circulation and Medical Imaging, Trondheim, Norway

[2] Department of Radiology and Nuclear Medicine, St. Olavs Hospital, Trondheim, Norway

* Corresponding author: albertina.rusandu@ntnu.no

Received: 3. 8. 2022
Accepted: 14. 10. 2022
https://doi.org/10.47724/MIRTJ.2022.i01.a001

ABSTRACT

Objectives: The aim of this study was to evaluate the effect of the choice of kernel on the image quality in abdominal CT images with a focus on liver lesion visibility.

Methods: In this comparative study, 84 abdominal CT examinations of patients with liver lesions that included parallel series reconstructed with two different kernels (B30 and B45) were analysed. A subjective assessment of image quality was performed using visual grading analysis based on anatomical criteria, liver lesion visibility and perceived image quality. Objective image quality was assessed using measurements of Hounsfield unit (HU) values (average and standard deviation) in abdominal organs and calculations of contrast-to-noise ratios (CNR).

Results: B30 kernel performed significantly better than B45 in all criteria except for sharpness. The most considerable improvement of the image quality was in terms of subjective experienced image noise, overall diagnostic image quality and visually sharp reproduction of liver lesions. The physical measurements showed that CNR increased by up to 46% when using B30.

Conclusions: Using a B30 kernel algorithm for image reconstruction reduces noise and thus improves image quality and diagnostic accuracy significantly relative to B45.

Key words: kernel, image quality, CT, noise reduction, liver lesions

Introduction

In computer tomography (CT) examinations, image quality depends on scanning parameters, reconstruction technique and parameters, together with scanners particularities. One of the factors that affect image quality and particularly image noise is the image reconstruction algorithm, also referred to as kernel. In filtered back projection (FBP)-based image reconstruction, images are obtained by filtering the projection data using a reconstruction kernel and then back projecting the filtered data to the image space (1). The kernels incorporate noise reduction, spatial resolution- and edge-increasing techniques that are applied to the raw data resulting from CT scanning. The choice of kernel always implies a trade-off between image noise and sharpness (spatial resolution) (2). CT images can be reconstructed multiple times with no additional radiation dose to the patient.

Different manufacturers operate with different designations for the kernels available on their CT-scanners. For example, GE uses more descriptive denominations (with kernels names like soft, detail, standard, bone, etc.) while others use codes (Phillips uses alphabetic denominations, Siemens uses codes, such as B30, B40, B45, B80, etc., while Toshiba uses FC08, FC12, FC30, etc.).

The detection and characterization of small focal lesions in parenchymal organs represent a challenge for the diagnostic radiologist and can have significant importance for a patient's further treatment. Reconstruction algorithms have an impact on image quality, i.e. to determine if adjustments in kernel reconstructions can improve the detection of parenchymal lesions.

Although iterative reconstruction (IR) is increasingly used as a result of its radiation dose reduction potential, FBP is still widely applied internationally due to some potential disadvantages of IR. These include increased implementation cost due to necessary purchases for every scanner or the inability to adopt this method at all because of older, incompatible scanners (1). Another disadvantage of IR is the usual change in noise texture compared to FBP images with which radiologists are more familiar, which may alter the radiologist satisfaction with the images and diagnostic confidence (3). Another reason FBP is still used is that applying the same reconstruction technique makes it is easier to compare with previous images. The purpose of this study was to evaluate the effect of the choice of kernel on the image quality in abdominal CT images with a focus on liver lesion visibility.

Material and methods

The CT scanners used in this study were Somatom Definition AS+ (128 slice), Somatom Definition Flash (2 x 128) and Somatom Sensation 64 (Siemens Medical Solutions, Forchheim, Germany). For a period of one year, all abdominal CT examinations included parallel series reconstructed with two different kernels (B30 and B45) in order to make it easier to compare the images with previous examinations. All examinations that showed liver lesions were included in the study (n=84). A post-hoc power analysis confirmed that the sample size was appropriate for detecting differences in image quality with a power of 80%.

Only the portal venous phases were evaluated. Scan timing was individualized using bolus-tracking with a threshold of 150 Hounsfield units (HU) in a region of interest (ROI) in the abdominal aorta on an axial image through the middle of the liver. The arterial phase was acquired using a delay of 25 seconds after reaching the threshold, and portal venous phase was acquired 30 seconds after the arterial phase. Iohexol (Omnipaque 350 mgI/ml, GE Healthcare) followed by 30 ml of saline was administered through an 18-gauge cannula placed in an antecubital vein. The contrast agent amount and flow were tailored to patient weight (<50 kg 120 ml and 3.2ml/s; 50–79 kg 150 ml and 4 ml/s; and >80 kg 180 ml and 4.8ml/s). The injection time was 37.5 s for all patients.

All examinations were performed at 120 kVp using automated tube current modulation (CareDose4D, Siemens) with 240 reference mAs. Pitch was set to 0,6 and the rotation time was 0.5 s/rotation. Both subjective and objective assessments of image quality were performed on images from the portal venous phase.

Patients' gender and age were retrieved from Picture Archiving and Communicating System (PACS) and, in order to compensate for the lack of information about patients' height and weight, effective diameter (eq 1) was used as an indicator for body habitus.

$$\text{Effective diameter} = \sqrt{anteroposterior\ diameter \times lateral\ diameter}$$

(eq 1)

Subjective assessment of image quality

The images were evaluated by two radiologists (with 5 and 12 years of experience) using relative visual grading analysis (VGA). The two image series were randomly displayed on the left and right monitor in PACS. A Sectra IDS7 (Linkoping, Sweden) PACS workstation with two diagnostic Eizo Radiforce MX241W monitors (Cypress, CA, USA) was used for image evaluation. The monitors' luminance was 320 cd/m^2, and the measurements were performed at a distance of 50–60cm from the monitor in an ambient lighting of 40–50lux. The radiologists evaluated the images independently, blinded to reconstruction kernel and without knowledge of the results of the physical measurements performed on the images. Radiologists were free to use all the tools available in PACS that are commonly used for clinical images (adjustment of window/level, magnification, etc.).

Table 1: Quality criteria used for visual image assessment

C1: visually sharp reproduction of the liver parenchyma
C2: visually sharp reproduction of the intrahepatic vessels
C3: visually sharp reproduction of liver lesions
C4: visually sharp reproduction of the spleen parenchyma
C5: visually sharp reproduction of the pancreas
C6: visually sharp reproduction of the kidneys and proximal ureters
C7: visually sharp reproduction of lymph nodes smaller than 15 mm in diameter
C8: image noise
C9: overall sharpness
C10: total assessment of diagnostic image quality

The criteria used in VGA (Table 1) were visualization of liver lesions (C3), perceived image quality (C8–C10) and a selection of anatomical criteria (C1–C2, C4–C7) from the European Guidelines on quality criteria for computed tomography (4).
The '2 / -2' rating (Table 2) was used when the radiologists thought it could have diagnostic consequences, for example that one could overlook or not completely evaluate something seen on one of the images when looking at the corresponding image reconstructed with the other kernel.

Table 2: Scoring

−2: Images on left monitor are much better than images on right monitor
−1: Images on left monitor are better than images on right monitor
0: Images on left and right monitor are equivalent
+1: Images on right monitor are better than images on left monitor
+2: Images on right monitor are much better than images on left monitor

The results from the VGA were summarized using VGA scores (VGAS) (5) for every criterion calculated using equation 2.

$$\text{VGAS}=\frac{\sum_{o,i} S_c}{N_i N_0} \qquad \text{(equation 2)}$$

where Sc represents the given individual scores for observer (o) and image (i), Ni represents the total number of images, and No represents the total number of observers.

Objective assessment of image quality

Attenuation (quantified as average HU) and noise (quantified as standard deviation HU) were measured in ROIs of approximately 12 mm in diameter placed on axial slices in paravertebral muscle, liver parenchyma, liver lesions, spleen, pancreas, aorta and fat tissue (Figure 1). To standardize measurements, ROIs were then copied and pasted on corresponding images reconstructed with the other kernel.
CNR values were calculated using the following equation (6):

where CNR represents $(HU_{Organ} - HU_{Muscle}) / SD_{Muscle}$,

CNR for liver lesions were calculated using the following equation (6):

where CNR represents $(HU_{liver} - HU_{Lesion}) / SD_{Muscle}$

Noise difference was calculated using the equation (6):

$$\text{Noise difference} = \frac{noise\,45 - noise\,30}{noise\,45} \times 100$$

where noise 45 and noise 30 is the SD measured in the liver on the images reconstructed with B45 kernel and B30 kernel, respectively.

Statistical analysis

Statistical analyses were conducted using SPSS for Windows version 27 (IBM Inc., Armonk, NY). The highlighted factors related to the distribution of data were: average, standard deviation, and lowest and highest value. The Shapiro–Wilk test was used to determine whether the data were normally distributed. Differences in physical image quality parameters between the groups were evaluated using a paired t-test. Differences in scores for subjective image quality were assessed using the Wilcoxon signed-rank test, while correlations between measured image quality parameters and criteria-based evaluations were analysed using Spearman's rank order. Inter-rater agreement was assessed using the weighted Cohen's kappa test with the following interpretation of agreement: 0.00–0.20 slight; 0.21–0.40 fair; 0.41–0.60 moderate; 0.61–0.80 substantial; and 0.81–1.00 almost perfect (7). Detailed analyses of percentage agreement were also used.

Ethical considerations

Institutional ethics review board approval was obtained (Research Committee of the Department of Medical Imaging at St. Olavs Hospital nr. 202012/21.04.2020). Written informed consent was waived due to the study's retrospective design. No personally identifiable information was recorded.

Results

A total of 84 examinations were assessed. Patient characteristics are presented in Table 3.

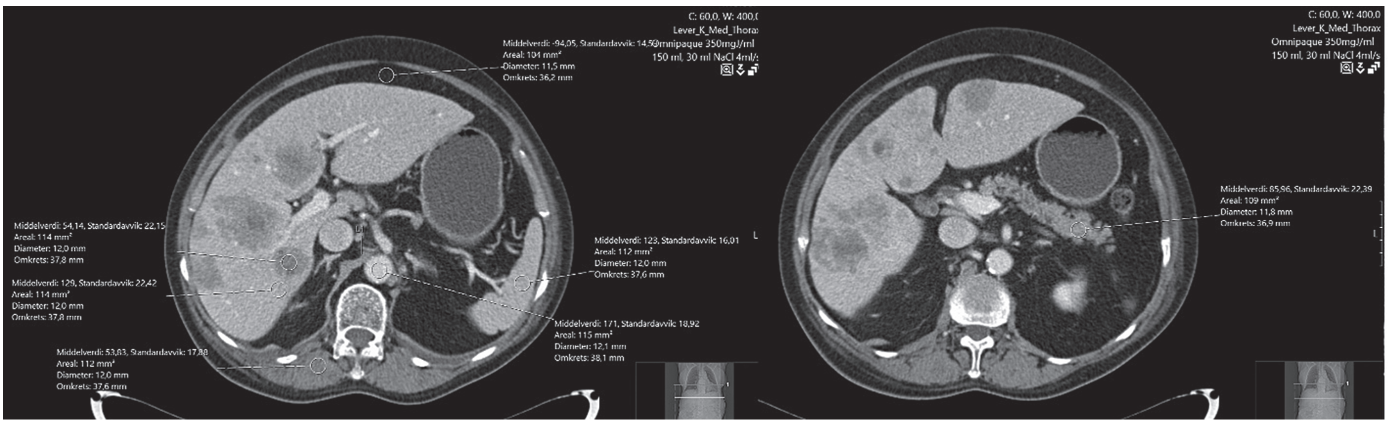

Figure 1: ROIs for the objective measurements of attenuation (quantified as average HU) and noise (quantified as standard deviation HU)

Table 3: Patient characteristics presented as average ± standard deviation (minimum – maximum)

Age	Gender (male/female ratio)	Effective diameter
64.47 ± 13.3 (35-89)	41/43	294 ± 38.3 (205-399)

Subjective assessment of image quality

The image quality differences made B30 the most preferred kernel option, and that kernel performed significantly better than B45 in all criteria except for overall sharpness (C9). These results are in line with the VGAS for each criterion that show the magnitude of the difference between kernels (Table 4) and the percentual distribution of difference evaluation scores (ure 2). The difference in favour of B30 is consistent and statistically significant.

The VGAS show that the most considerable improvement of the image quality when using B30 instead of B45 is in terms of subjective experienced image noise, overall diagnostic image quality and the visually sharp reproduction of liver lesions, while the effect on the reproduction of lymph nodes smaller than 15 mm in diameter is least significant. The differences in image quality between the two kernels were statistically significant for all criteria ($p<0.001$ for difference analysed using the Wilcoxon signed-rank test).

In almost 30% of cases, the images reconstructed with the B30 kernel were considered much better than the images reconstructed with the B45 kernel (Figure 2).

There was high level of agreement between the two radiologists regarding the preferred kernel for all criteria, with the exception of the visually sharp reproduction of the liver parenchyma and overall sharpness. However, in terms of the magnitude of the image quality difference between the two kernels, there was only fair inter-observer agreement (κ in the range of 0.2–0.4).

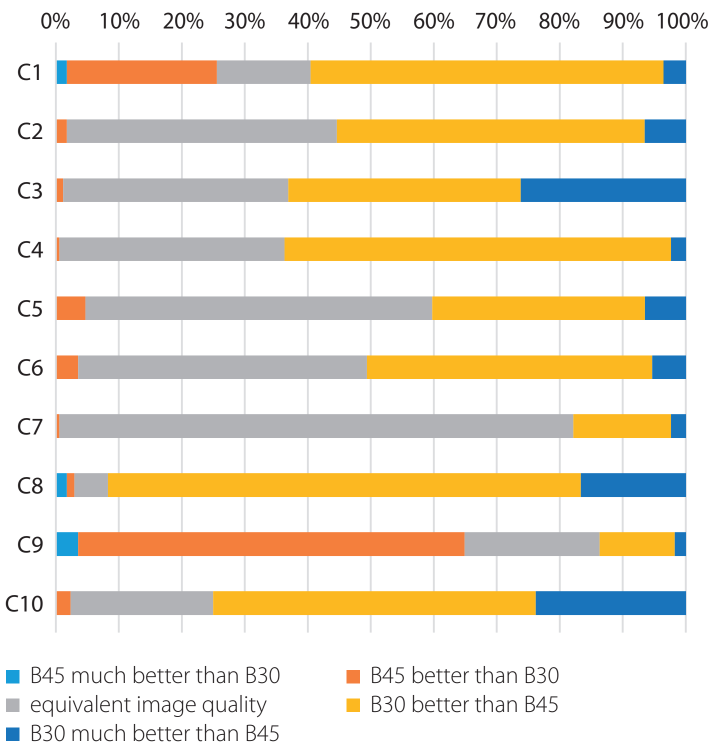

Figure 2: Comparison of the images reconstructed with the two kernels

Table 4: Results of criteria-based image quality comparation for B30 and B45 reconstruction kernels presented as VGA scores, preferred option, and percent agreement between the radiologists regarding preferred kernel

Criteria*	VGAS (B30>B45)	Preferred kernel	Percent agreement
C1	0.345	B30	67
C2	0.601	B30	96
C3	0.880	B30	98
C4	0.655	B30	99
C5	0.423	B30	98
C6	0.524	B30	95
C7	0.196	B30	99
C8	1.036	B30	94
C9	-0.529	B45	39
C10	0.964	B30	95

* C1 visually sharp reproduction of the liver parenchyma, C2 visually sharp reproduction of the intrahepatic vessels, C3 visually sharp reproduction of liver lesions, C4 visually sharp reproduction of the spleen parenchyma, C5 visually sharp reproduction of the pancreas, C6 visually sharp reproduction of the kidneys and proximal ureters, C7 visually sharp reproduction of lymph nodes smaller than 15 mm in diameter, C8 image noise, C9 overall sharpness, and C10 total assessment of diagnostic image quality

Objective assessment of image quality

Noise levels measured in all organs were substantially lower and CNR considerably higher for the B30 kernel (Table 5). The differences were statistically significant and the percentual differences were around 45% in all organs.

The correlation between the subjective assessed score for image noise and measured noise in the liver, spleen and muscle was statistically significant. The correlation between the subjective evaluation of the reproduction of liver lesions and the measured image noise both in the liver and in liver lesions was statistically significant.

Discussion

This study compared abdominal CT scans reconstructed with two different kernels in routine clinical settings. B30 was the preferred kernel in this study for all criteria except for one and for the overall image quality. The difference in both measured image quality parameters and subjective image quality assessment between B30 and B45 were statistically significant for all criteria.

As expected, the results show a difference in both measured and perceived image noise, which was significantly lower in B30 images. Image noise reduction is proven to result in higher confidence in lesion detection (8). This is confirmed by the correlation between the assessment of the reproduction of liver lesions and measured image noise in the liver in

Table 5: Average values and standard deviations for image quality parameters measured for the two kernels and percentual difference (p<0.001 for all parameters in all organs)

	B30		B45		Percentual difference (%)	
	Noise (SD in HU)	CNR	Noise (SD in HU)	CNR	Noise (SD in HU)	CNR
Liver	15.43±3.49	4.63±1.52	28.87±6.41	2.51±0.74	46.6	45.78
Liver lesion	16.81±4.50	4.55±2.25	30.30±7.93	2.43±1.19	44.52	46.59
Spleen	15.01±3.01	4.70±1.64	28.66±5.66	2.56±0.86	47.63	45.53
Pancreas	18.41±4.38	3.01±1.44	32.29±8.42	1.64±0.79	42.99	45.51
Aorta	16.71±3.76	8.59±2.64	29.90±7.20	4.69±1.45	44.11	45.40
Muscle	15.55±3.57	-	28.44±6.37	-	45.32	

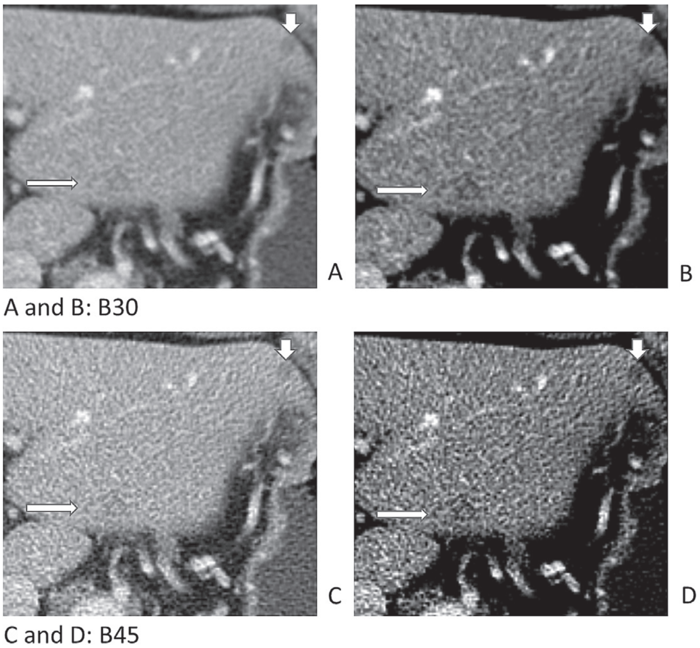

Figure 3: The figure shows two different window settings in A and B for the B30 kernel reconstruction, C and D for B45 of the CT images of this 62-year-old patient with primary neuroendocrine tumour of the small intestine (window levels are C:50, W:380 in A and C, C: 120, W: 200 in B and D). Two small liver lesions are shown in the left liver. The one anteriorly (thick arrow) is quite easy to see in all reconstructions. The other lesion (thin arrow) more posteriorly and medially is difficult to see. A change in window level helps the demarcation in the B30 algorithm. In the B45 reconstruction, the noise makes it much harder to detect it in both window settings.

our study (Figure 3). The image noise reduction obtained using B30 instead of B45 (Table 5) was higher than the value obtained by Bhosale et al. (9) when comparing a soft kernel and standard kernel.

B45 performed better than B30 for overall sharpness (C9). The importance of sharpness depends on the diagnostic task, while the assessment of its clinical relevance is beyond the scope of this paper. Sharpness, however, is most relevant for demarcation in areas with high contrast, such as parenchyma against fat. Internal parenchymal structures, such as lobes or subtle contrast heterogeneities, are better depicted in B30 images (Figure 4). Therefore, the overall diagnostic image quality scores show that B30 was much better than B45 in almost 30% of cases. This, together with a low percent

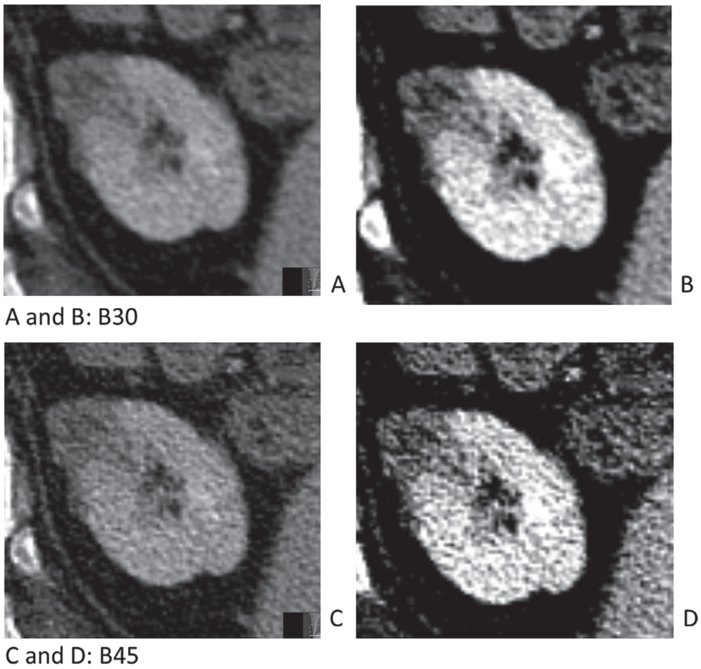

Figure 4: This 52-year-old patient had a primary thymus malignancy with metastasis to the left kidney. A and B are a B30, C and D a B45 reconstruction. A and C are shown with a soft tissue window level C:160, W:450, B and D in window level C: 120, W: 200. While the metastatic lesion is somewhat more sharply demarcated in the B45 kernel reconstruction (right), the subtle internal structure of both tumour tissue as well as kidney parenchyma is much better on B30 reconstructed images.

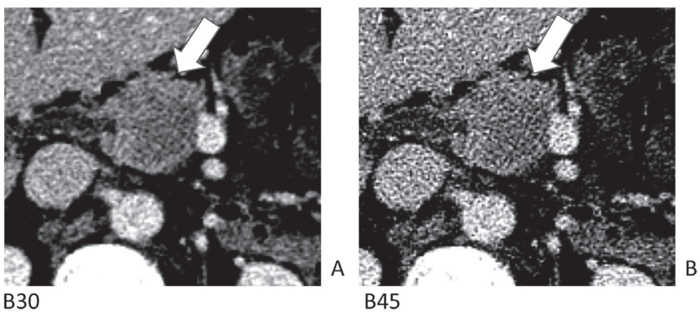

Figure 5: This 52-year-old patient had a primary thymus malignancy with metastasis to the head of the pancreas (same patient as in Figure 4, window level C: 120, W: 200). In A, the reconstruction kernel is B30, while in B it is B45. The edge of the metastasis and subtle tissue structure of the surroundings are blurred by the noise on reconstructions with B45.

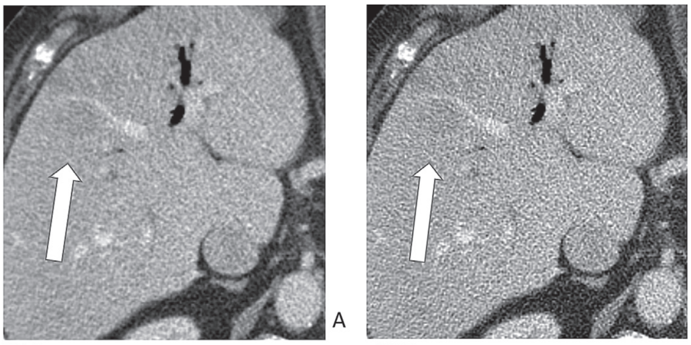

***Figure 6:** An 82-year-old patient with a duodenal malignancy obstructing the papilla vateri, with metastatic liver disease. Air in the intrahepatic biliary tree after Endoscopic retrograde cholangiopancreatography (ERCP) with stenting. The patient was inoperable due to comorbidity. Metastases to the liver are clearly more visible on the B30 kernel reconstruction (A) compared to B45 (B), window level C:50, W: 380*

agreement between the radiologists when scoring overall sharpness and no significant correlation between this criterion in either the visually sharp reproduction of liver lesions or overall diagnostic image quality, suggests that the clinical relevance of the lower overall sharpness when using B30 might be negligible.

The considerable differences in CNR and quality assessment scores indicate the much better visually detectable reproduction of liver lesions in B30 and suggest that the increased image noise due to the choice of B45 might obscure small low-contrast lesions (Figure 5). At first glance, the sharp images often seem better, but when analysing the organs in more detail, the demarcation between parenchyma and pathology is sometimes blurred by noise on B45 reconstructions (Figure 6). This is especially true for small parenchymal lesions. The reason is the sacrifice of low contrast resolution due to particular image filtering and the post-processing technique, which increase the image noise when choosing a sharp kernel that gives better spatial resolution (1). It seems that a sharp kernel makes what is already obvious even more obvious. However, fine diagnostics are convincingly better with a softer kernel that gives better texture at the edge of metastases (Figure 5). Other criteria with high VGAS were subjective evaluated noise (C8) and overall diagnostic image quality (C10) (Table 4).

In the pancreas (C5), delimitation against fat looks better on B45 at first glance. However, in patients with low BMI, the delineation of organs' contours can be difficult on images with high noise level due to the low amount of intra-abdominal fat (10), while blurred lesions become more pronounced on B30, which is crucial in severe pathology. That gave a slight difference in image quality with regard to C5 (a VGAS of 0.423 out of a maximum possible 2 points).

The correlation between lower levels of measured image noise in the organs on the B30 images and the subjective assessed scores was statistically significant. However, not all the measurements correlated with the scores given by the radiologists, which might be explained by the fact that some anatomical structures may be more important than others for the anatomical region or pathology being investigated. More studies are required in this area to identify the weighting factors of the criteria, depending on the clinical indication (11).

The kappa values indicate some inter-observer differences. This difference might be caused by the difficulty in obtaining identical scores when a large scoring scale is used (12) or the different use of viewing tools, but it might also be an underlying difference between the reader's image quality expectancy or the fact that reader's preference scale might also change during the reading session which is described in literature as adaptation (13). VGA results when visualizing different noise textures might also be influenced by the experience of the radiologist (5). Another reason for the low kappa might be the ambiguity of the criteria, i.e. the sharp reproduction of the liver that might be subject to interpretation (it is worth noting that the percent agreement was also lower for C1) or difficulty in scoring normal anatomy with regard to diagnostic quality in the absence of pathology in the assessed organ. The use of image quality criteria stated in European guidelines is recommended for optimizing CT protocols based on the assumption that sharply reproduced anatomy results in sharply reproduced pathology. However, the relationship between the reproduction of anatomy and the detection of pathology is still unclear and further studies are needed, including an analysis in which pathology is taken into consideration to evaluate the relationship between image quality and diagnostic efficacy (10, 14). Similar kappa values were reported in studies using similar image quality assessment methods (10). However, the extent of differences showed by the kappa values is not confirmed by the percentual agreement which was over 90 for most of the criteria, while percentual agreement is considered a more informative agreement measure for clinicians (15).

The present study is subject to several limitations. 1. A statistically significant difference in image quality assessment results does not necessarily mean a difference in diagnostic performance. However, because CNR is considered a significant predictor for lesion detection, (16) image noise reduction may result in higher confidence in lesion detection. 2. Despite the randomization of the images, a truly blinded comparison was impossible due to the noticeable differences in image noise between the images reconstructed with the two kernels. 3. Only kernels from one vendor and only portal venous phase images were evaluated. 4. VGAS was the only scoring system used for quantifying the criteria-based image quality assessment. However, VGAS is still widely used to demonstrate the magnitude of the difference between options and providing a context to interpret the physical measurements (5) despite their shortcomings (17, 18), while a Wilcoxon test value is equal to the area under the curve (AUC) in a receiver operating characteristics (ROC) analysis of the same data (19).

Conclusion

The comparative image quality assessment demonstrates the superiority of B30 over B45 kernel reconstruction in abdominal CT examinations. This approach provides a statistically significant reduction in image noise, and an increase in CNR and higher VGA scores for all criteria except for overall sharpness. With the main goal of achieving the highest subjective sensitivity for detecting focal lesions, the criterion "sharpness" proved to be a secondary factor in this study and is negligible.

References

1. Ehman EC, Yu L, Manduca A, Hara AK, Shiung MM, Jondal D, et al. Methods for clinical evaluation of noise reduction techniques in abdominopelvic CT. Radiographics. 2014;34(4):849-62. https://doi.org/10.1148/rg.344135128

2. Bushberg JT. The essential physics of medical imaging. 3rd ed. ed. Philadelphia: Wolters Kluwer Health/Lippincott Williams & Wilkins; 2011.

3. Fletcher JG, Krueger WR, Hough DM, Huprich JE, Fidler JL, Wang J, et al. Pilot study of detection, radiologist confidence and image quality with sinogram-affirmed iterative reconstruction at half-routine dose level. J Comput Assist Tomogr. 2013;37(2):203-11. DOI: 10.1097/rct.0b013e31827e0e93

4. Jessen K, Shrimpton P, et al., Panzer W. European guidelines on quality criteria for computed tomography. Luxembourg: Luxembourg: OPOCE; 2000.

5. Verdun FR, Racine D, Ott JG, Tapiovaara MJ, Toroi P, Bochud FO, et al. Image quality in CT: From physical measurements to model observers. Physica Medica. 2015;31(8):823-43. https://doi.org/10.1016/j.ejmp.2015.08.007

6. Eichler M, May M, Wiesmueller M, Saake M, Heiss R, Uder M, et al. Single source split filter dual energy: Image quality and liver lesion detection in abdominal CT. European Journal of Radiology. 2020;126:108913. https://doi.org/10.1016/j.ejrad.2020.108913

7. Landis JR, Koch GG. The Measurement of Observer Agreement for Categorical Data. Biometrics. 1977;33(1):159-74. PMID: 843571

8. Goenka AH, Herts BR, Dong F, Obuchowski NA, Primak AN, Karim W, et al. Image Noise, CNR, and Detectability of Low-Contrast, Low-Attenuation Liver Lesions in a Phantom: Effects of Radiation Exposure, Phantom Size, Integrated Circuit Detector, and Iterative Reconstruction. Radiology. 2016;280(2):475-82. https://doi.org/10.1148/radiol.2016151621

9. Bhosale PW-B, Nicolaus; Wei Wei; Kundra, Vikas; Tamm, Eric. Comparing CNR, SNR, and Image Quality of CT Images Reconstructed with Soft Kernel, Standard Kernel, and Standard Kernel plus ASIR 30% Techniques. International Journal of Radiology. 2016;2(2). http://www.ghrnet.org/index.php/IJR/article/view/1101/1773

10. Kataria B, Althén JN, Smedby Ö, Persson A, Sökjer H, Sandborg M. Assessment of image quality in abdominal CT: potential dose reduction with model-based iterative reconstruction. Eur Radiol. 2018;28(6):2464-73. DOI: 10.1007/s00330-017-5113-4

11. Zarb F, Rainford L, McEntee MF. Image quality assessment tools for optimization of CT images. Radiography. 2010;16(2):147-53. https://doi.org/10.1016/j.radi.2009.10.002

12. McHugh ML. Interrater reliability: the kappa statistic. Biochem Med (Zagreb). 2012;22(3):276-82. PMID: 23092060

13. Helson H. Adaptation-level theory. Oxford, England: Harper & Row; 1964. xvii, 732-xvii

14. Jurik A, Petersen J, Jessen KA, Bongartz G, Geleijns J, Golding SJ, et al. Clinical Use of Image Quality Criteria in Computed Tomography: A Pilot Study. Radiation Protection Dosimetry. 2000;90(1-2):47-52. https://doi.org/10.1093/oxfordjournals.rpd.a033142

15. de Vet HCW, Mokkink LB, Terwee CB, Hoekstra OS, Knol DL. Clinicians are right not to like Cohen's κ. BMJ : British Medical Journal. 2013;346:f2125. https://doi.org/10.1136/bmj.f2125

16. Baker ME, Dong F, Primak A, Obuchowski NA, Einstein D, Gandhi N, et al. Contrast-to-Noise Ratio and Low-Contrast Object Resolution on Full- and Low-Dose MDCT: SAFIRE Versus Filtered Back Projection in a Low-Contrast Object Phantom and in the Liver. American Journal of Roentgenology. 2012;199(1):8-18. https://www.ajronline.org/doi/10.2214/AJR.11.7421

17. Båth M. Evaluating imaging systems: practical applications. Radiation Protection Dosimetry. 2010;139(1-3):26-36. https://pubmed.ncbi.nlm.nih.gov/20147386/

18. Månsson LG. Methods for the Evaluation of Image Quality: A Review. Radiation Protection Dosimetry. 2000;90(1-2):89-99. https://doi.org/10.1093/oxfordjournals.rpd.a033149

19. Precht H, Hansson J, Outzen C, Hogg P, Tingberg A. Radiographers' perspectives' on Visual Grading Analysis as a scientific method to evaluate image quality. Radiography. 2019;25:S14-S8. https://doi.org/10.1016/j.radi.2019.06.006